Progress In Electromagnetics Research Letters, Vol. 50, 49–54, 2014

A Compact Triple-Band Passband Filter Using Multi-Stub Loaded Resonator and Asymmetrical SIRs

Jun-Mei Yan[1, 2, *], Liang-Zu Cao[1, 2], and Xing-Guo Wang[1]

Abstract—This letter presents a compact triple-band passband filter with high frequency selectivity. The first and second passbands are formed by a multi-stub loaded resonator. The bandwidth of the second passband can be independently adjusted by tuning the coupling strength between the two loaded open stubs. The third passband is implemented using two asymmetrical stepped impedance resonators (SIRs) with a tapped line structure as external coupling form. The asymmetrical SIRs also serve as one part of the external coupling structure of the multi-stub loaded resonator so as to achieve a compact circuit size. Additionally, a source-load coupling is introduced, thus, multiple transmission zeros are generated to improve the frequency selectivity. After a detailed introduction of the operation principle, a triple-band passband filter with centre passband frequencies of 1.5, 2.6 and 3.6 GHz is designed and fabricated. The measured results verify the effectiveness of the proposed filter.

1. INTRODUCTION

As key components of the multi-band wireless service system, the multi-band passband filters have been extensively studied for past decades. They should have a compact size, flexible design freedom, high frequency selectivity and sufficient suppression of the parasitic harmonic modes. Many approaches have been utilized to implement multi-band filters. The most common method is based on SIRs [1-3], whose first two resonant modes can be controlled by properly selecting the relevant impedance or strip width ratio. But this method often suffers from a large circuit size and limited design freedom. The stub loaded multi-mode microstrip resonator [4–7] and the degenerate modes of perturbed ring resonators [8–14] can also be utilized to construct multi-band filters. In [15], the multi-stub loaded resonator was used to implement a dual-band passband filter with independently controlled bandwidth by inserting a half-wavelength resonator between the loaded open stubs so as to introduce two signal paths. The transmission zeros generated by the direct source-load coupling improved the isolation between the passbands greatly and suppressed the parasitic harmonic modes to achieve a wider upper stopband. Following [15], in this letter, a compact triple-band passband filter with high frequency selectivity is proposed, whose first two passbands are implemented using the multi-stub loaded resonator in [15]. The third passband is formed by using two asymmetrical electronically coupled SIRs. The SIR has a tapped line structure as the external coupling form. Simultaneously, as one part of the input/output structure of the multi-stub loaded resonator, the SIR not only accomplish the external coupling of the multi-stub loaded resonator, but also can introduce source-load coupling to improve frequency selectivity. Thus, the multi-stub loaded resonator combined with two SIRs achieves triple-band passband filtering function, while the circuit size does not increase considerably. Structure and design of the filter are in detail introduced in the remainder. A triple-band passband filter with center frequencies of 1.5, 2.6 and 3.6 GHz is fabricated and measured. The measured results verify the effectiveness of the proposed filter.

Received 5 October 2014, Accepted 3 November 2014, Scheduled 23 November 2014

* Corresponding author: Jun-Mei Yan (yjmzhy@163.com).

[1] School of Mechanical and Electronic Enginerring, Jingdezhen Ceramic Institute, China. [2] School of Electronic and Optical Engineering, Nanjing University of Science and Technology, China.

2. STRUCTURE AND DESIGN

Shown in Fig. 1 is the configuration of the proposed triple-band passband filter. The filter is designed on a substrate with thickness of 0.8 mm, dielectric constant of 2.55 and loss tangent of 0.0004. Just like the multi-stub loaded resonator in [15], the uniform impedance half-wavelength resonator ($2(L_1 + L_2 + L_3 + L_4)$) is loaded with two open microstrip lines ($L_8 + L_9 + 2L_{10} + L_{11}$) and a shorted stub ($L_0$). For a compact circuit size, in our proposed filter, a direct coupling between the two open microstrip lines through gap g_3 replaces the corresponding coupling, in [15], generated by adding an extra resonator. Two asymmetrical stepped impedance resonators (SIRs) ($L_5 + L_6 + L_7$) are embedded within the multi-stub loaded resonator, by which the third passband is formed with the tapped line structure as the external coupling form and open parallel coupling microstrip lines (L_5, W_3, g_2) accomplishing inter-resonator coupling. Additionally, for the multi-stub loaded resonator, the SIRs provide input/ouput coupling through the gap g_1 and direct source-load coupling through open parallel coupling microstrip lines.

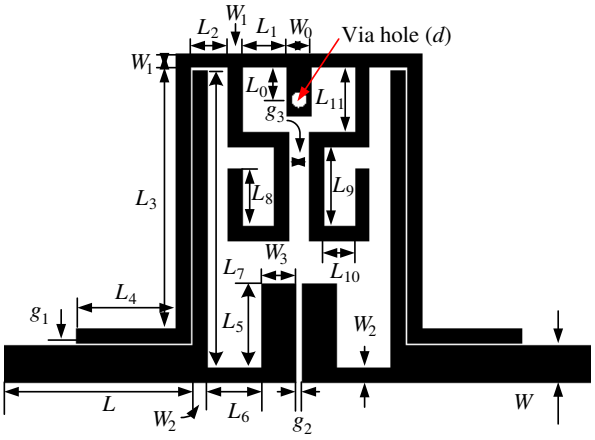

Figure 1. Configuration of the proposed triple-band passband filter.

Inset (a) of Fig. 2 shows the transmission line model of the asymmetrical SIR along with the tapped line structure. According to the transmission line model, the following equations hold,

$$Y = Y_1 + Y_2 \tag{1}$$

$$Y_1 = j\frac{1}{Z_1}\tan\theta_1 \tag{2}$$

$$Y_2 = \frac{j(Z_1\tan\theta_3 + Z_2\tan\theta_2)}{Z_1Z_2 - Z_1^2\tan\theta_1\tan\theta_3} \tag{3}$$

where, Y is the input admittance at the tapped point, Y_1 the admittance seen left from the tapped point, and Y_2 the admittance seen right. The resonance occurs at frequencies where $Y = 0$. The resonant frequency changes against different impedance ratios of Z_2/Z_1 and different electrical lengths of $\theta_1 + \theta_2$. Fig. 3 shows the details. It is noted that the electrical length values ($\theta_1 + \theta_2$) are referenced to frequency of 3.5 GHz, and the total electrical length ($\theta_1 + \theta_2 + \theta_3 = 180°$) keeps unchanged. Therefore, the resonance can be easily aligned within the third passband.

To extract the external quality factor, the reflection coefficient is computed using (4), in which Y_0 is the internal admittance of the source.

$$S_{11} = \frac{Y_0 - Y}{Y_0 - Y} \tag{4}$$

$$Q_e = \frac{\omega_0}{\Delta\omega_{\pm 90°}} \tag{5}$$

The phase information of S_{11} is utilized to get the external quality factor Q_e using (5) [16]. In (5),

$\Delta\omega_{\pm 90^\circ}$ is the absolute bandwidth between the $\pm 90^\circ$ phase points. Thus, the external quality factor for different impedance values of Z_1, Z_2 and different electrical length values of θ_1 can be obtained.

Fig. 2 shows the simulated insertion loss for only the third passband (responding to the inset (b) of Fig. 2) against different gaps g_2. A smaller g_2 results in a stronger inter-resonator coupling, which will generates a wider bandwidth. The simulations, in the letter, are all carried out using Ansoft HFSS 14.0. From Fig. 2, the transmission zero (Tz) is observed, which is from the $Y_1 = \infty$ condition.

The multi-stub loaded resonator has already been discussed in detail in [15]. It can generate two passbands, here, used as the first and second passbands. The center frequency of the first and second passbands is mainly determined by the length of $L_0+L_1+L_2+L_3+L_4$ and $L_0+L_1+L_8+L_9+2L_{10}+L_{11}$. They form a quarter-wavelength resonator respectively. The center frequency can be separately adjusted. For the two passbands, their external coupling is accomplished by the fringe coupling of gap g_1, which cannot be tuned separately. The shorted stub L_0 provides a convenient internal coupling in the two passbands. A long L_0 will result in more obvious resonant modes splitting, which means a strong coupling. But it impacts the two passbands simultaneously, which is not desirable. Fortunately, tuning the gap g_3 can individually control the internal coupling in the second passband. In [15], the individually controlled coupling is generated by adding an extra resonator between the loaded microstrip lines. So a compact circuits size is achieved here.

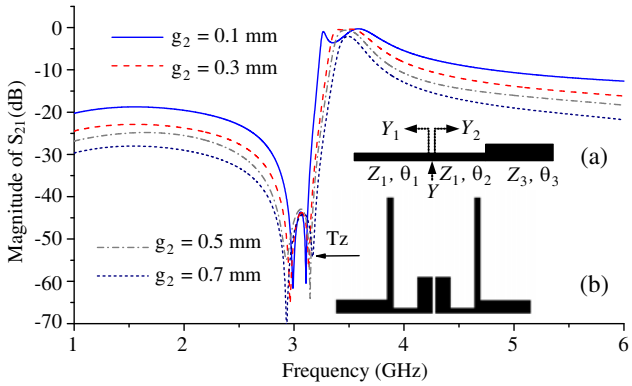

Figure 2. Simulated results of the third passband formed by the two asymmetrical SIRs. (a) Transmission line model of the SIR, (b) simulation model, dimensions are $L_5 = 5.1$, $L_6 = 3.35$, $L_7 = 18.05$, $W = 2.2$, $W_2 = 0.8$, $W_3 = 2.0$. (All are in mm).

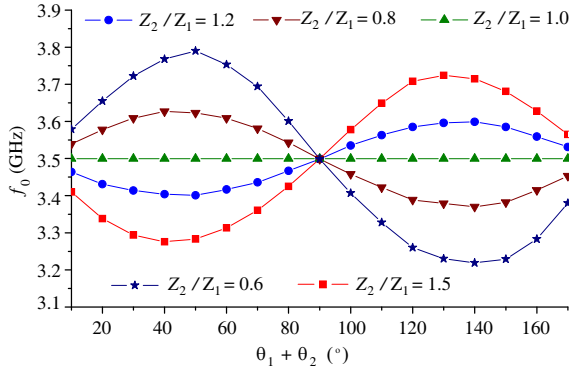

Figure 3. The resonance frequency of the asymmetrical SIR against different impedance ratio and electrical length with $\theta_1+\theta_2+\theta_3 = 180^\circ$ unchanged.

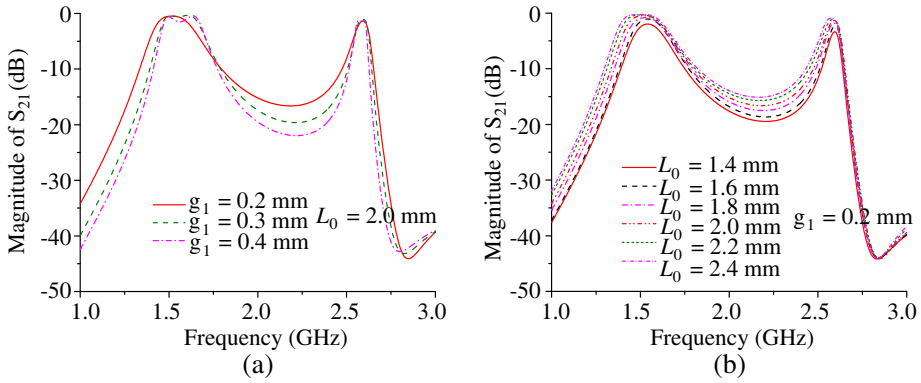

Figure 4. Simulated insertion loss against (a) different g_1 and (b) different L_0 for case with only the multi-stub resonator. Other dimensions are $W_0 = 1.5$, $W_1 = 0.8$, $L_1 = 2.7$, $L_2 = 2.35$, $L_3 = 15.9$, $L_4 = 6.05$, $L_8 = 3.5$, $L_9 = 4.9$, $L_{10} = 2.0$, $L_{11} = 4$, $g_3 = 1.3$, $d = 1.0$, (all are in mm).

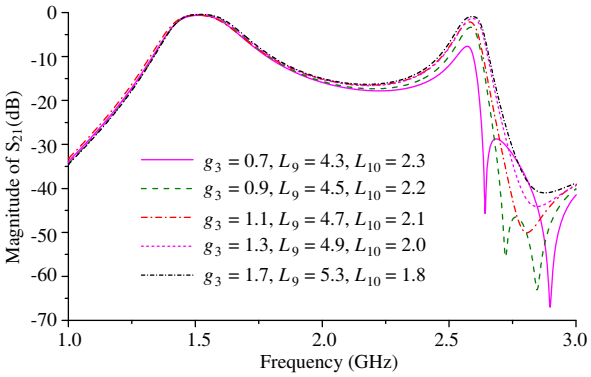

Figure 5. Simulated insertion loss against different g_3 with $L_8 + L_9 + 2L_{10} + L_{11} = 16.4$ mm unchanged for case with only the multi-stub loaded resonator. $g_1 = 0.2$, $L_0 = 2.0$ (all are in mm).

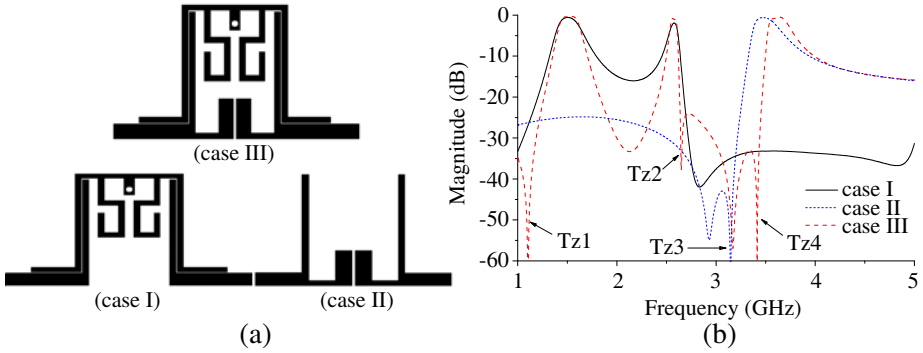

Figure 6. Comparison of the simulated insertion loss for three cases. (a) Simulation model for case I (with only multi-stub loaded resonator), case II (with only asymmetrical SIRs) and case III (with both multi-stub loaded resonator and asymmetrical SIRs), (b) simulated insertion loss for three cases.

Fig. 4 shows the simulated insertion loss against different g_1 and different L_0 for the case with only multi-stub loaded resonator, i.e., case I in Fig. 6(a). From Fig. 4(a), the bandwidths of two passbands change simultaneously for different g_1. It means that tuning g_1 can change the external couplings. The external coupling can also be tuned by changing the length of gap g_1. The simulated insertion loss shown in Fig. 4(b) indicates that L_0 affects internal coupling of two passbands simultaneously. Fig. 5 shows the simulated insertion loss against different values of g_3. Obviously, the bandwidth of the second passband can be independently adjusted in proper range by tuning g_3.

Fig. 6 shows the comparison of the simulated insertion loss in three cases. For case III (with multi-stub loaded resonator and SIRs), four transmission zeros (Tz1, Tz2, Tz3, Tz4) and an extra passband (the third passband) are generated in comparison with case I (with only multi-stub loaded resonator), which are obviously from the source-load coupling introduced by the embedded SIRs and tapped line structure. Additionally, for case III, the frequency selectivity between the first and second passbands is also improved. For the third passband, a frequency shift about 0.1 GHz in case III in comparison with case II (with only SIRs) is observed, which is from the loading effectiveness of the multi-stub loaded resonator to the SIRs.

3. EXPERIMENTAL RESULTS

Fig. 7 shows a photograph of the fabricated filter and the simulated and measured results. The universal test fixture (Anritsu 3680V) and vector network analyzer (Agilent N5224A) are used for measurement. From Fig. 7, although a little frequency shift exists, three passbands with the centre frequencies of 1.63, 2.64 and 3.61 GHz can be clearly observed. The relative large discrepancy between the simulated and

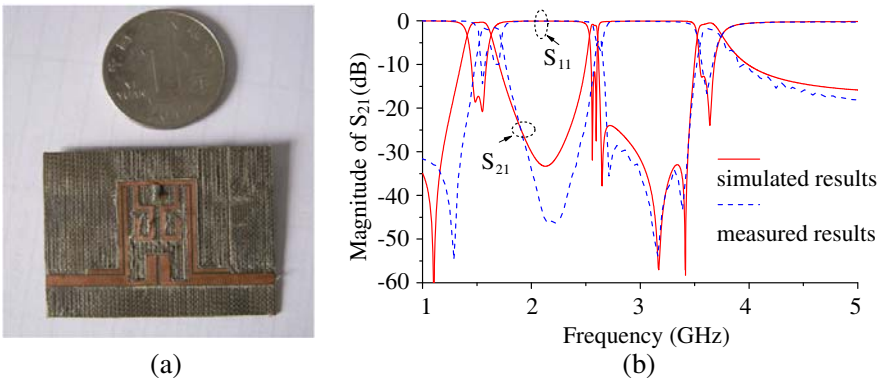

Figure 7. (a) Photograph of the fabricated filter and (b) the simulated and measured results.

measured results in the first two passbands exists, and it might be due to the unexpected tolerance of fabrication and implement. The physical dimensions of the fabricated filter are indicated in the captions of Fig. 2 and Fig. 4. The practical size is $26.9 \times 16.0\,\text{mm}^2$, about $0.21\lambda_g \times 0.12\lambda_g$, where λ_g is the guided wavelength at center frequency of the first passband.

4. CONCLUSION

This letter presents a compact triple-band passband filter implemented by embedding two asymmetrical SIRs within a multi-stub loaded resonator. Multiple transmission zeros are introduced to improve the frequency selectivity. The bandwidth of three passbands can be independently adjusted in a proper range. After the operation principle of the filter is described in detail, a prototype filter is fabricated and measured. The measured results verify the effectiveness of the proposed filter.

ACKNOWLEDGMENT

This work was supported by Science and Technology Support Program of Jiangxi Province of China (Grant Nos. 2012ZBBE50025).

REFERENCES

1. Chu, Q.-X. and F.-C. Chen, "A compact dual-band bandpass filter using meandering stepped impedance resonators," *IEEE Microw. Wireless Compon. Lett.*, Vol. 18, No. 5, 320–322, 2008.
2. Chu, Q.-X. and X.-M. Lin, "Advanced triple-band bandpass filter using tri-section sir," *Electron. Lett.*, Vol. 44, No. 4, 295–296, 2008.
3. Hsu, C.-I., C.-H. Lee, and Y.-H. Hsieh, "Tri-band bandpass filter with sharp passband skirts designed using tri-section sirs," *IEEE Microw. Wireless Compon. Lett.*, Vol. 18, No. 1, 19–21, 2008.
4. Chu, Q.-X., F.-C. Chen, Z.-H. Tu, and H. Wang, "A novel crossed resonator and its applications to bandpass filters," *IEEE Trans. Microw. Theory Tech.*, Vol. 57, No. 7, 1753–1759, 2009.
5. Chen, F.-C., Q.-X. Chu, and Z.-H. Tu, "Tri-band bandpass filter using stub loaded resonators," *Electron. Lett.*, Vol. 44, No. 12, 747–749, 2008.
6. Zhang, X. Y., C. H. Chan, Q. Xue, and B.-J. Hu, "Dual-band bandpass filter with controllable bandwidths using two coupling paths," *IEEE Microw. Wireless Compon. Lett.*, Vol. 20, No. 11, 616–618, 2010.
7. Gao, L., X. Y. Zhang, B. J. Hu, and Q. Xue, "Novel multi-stub loaded resonators and their applications to various bandpass filters," *IEEE Trans. Microw. Theory Tech.*, Vol. 62, No. 5, 1162–1172, 2014.

8. Huang, T.-H., H.-J. Chen, C.-S. Chang, L.-S. Chen, Y.-H. Wang, and M.-P. Houng, "A novel compact ring dual-mode filter with adjustable second-passband for dual-band applications," *IEEE Microw. Wireless Compon. Lett.*, Vol. 16, No. 6, 360–362, 2006.
9. Djoumessi, E. E. and K. Wu, "Multilayer dual-mode dual-bandpass filter," *IEEE Microw. Wireless Compon. Lett. I*, Vol. 19, No. 1, 21–23, 2009.
10. Luo, S. and L. Zhu, "A novel dual-mode dual-band bandpass filter based on a single ring resonator," *IEEE Microw. Wireless Compon. Lett.*, Vol. 19, No. 8, 497–499, 2009.
11. Wang, Y. X., B.-Z. Wang, and J. P. Wang, "A compact square loop dual-mode bandpass filter with wide stop-band," *Progress In Electromagnetics Research*, Vol. 77, No., 67–73, 2007.
12. Zhao, L.-P., X.-W. Dai, Z.-X. Chen, and C.-H. Liang, "Novel design of dual-mode dual-band bandpass filter with triangular resonators," *Progress In Electromagnetics Research*, Vol. 77, 417–424, 2007.
13. Wu, G.-L., W. Mu, X.-W. Dai, and Y.-C. Jiao, "Design of novel dual-band bandpass filter with microstrip meander-loop resonator and CSRR DGS," *Progress In Electromagnetics Research*, Vol. 78, 17–24, 2008.
14. Luo, S., L. Zhu, and S. Sun, "A dual-mode dual-band bandpass filter using a single slot ring resonator," *Progress In Electromagnetics Research Letters*, Vol. 23, 173–180, 2011.
15. Chen, F., Q. Chu, Z. Li, and X. Wu, "Compact dual-band bandpass filter with controllable bandwidths using stub-loaded multiple-mode resonator," *IET Microwaves, Antennas and Propagation*, Vol. 6, No. 10, 1172–1178, 2012.
16. Hong, J.-S. and M. J. Lancaster, *Microstrip Filter for RF/Microswave Applications*, John Wiley & Sons, 2001.